Platelet Mimetic Particles for Targeting Thrombi in Flowing Blood

Nishit Doshi[1,†], **Jennifer N. Orje**[2,†], **Blanca Molins**[2,§], **Jeffrey W. Smith**[3], **Samir Mitragorti**[1,*], and **Zaverio M. Ruggeri**[2,*]

[1]Department of Chemical Engineering, University of California, Santa Barbara, CA

[2]Department of Molecular and Experimental Medicine, The Scripps Research Institute, La Jolla, CA

[3]The Sanford-Burnham Institute, La Jolla, CA.

Keywords

platelets; targeted drug delivery; polymeric particles; layer-by-layer technique; GPIb; VWF domain

Mammalian platelets are anucleated cell fragments derived from megakaryocytes[1] that play a vital role in several physiologic and pathologic processes such as hemostasis and thrombosis[2], release of growth factors and modulation of inflammatory and immune responses[3]. The contribution to hemostasis, a process during which platelets have a key role in forming the plugs that seal injured vessels and arrest bleeding, is essential for the integrity of blood circulation [4, 5]. This complex function involves the ability to adhere to reactive subendothelial structures exposed at sites of injury and aggregate with one another in flowing blood[6]. To be efficient, this process must take place on both venular and arteriolar side of the circulation, the latter being where greatest is the physical challenge of overcoming the fluid dynamic forces that oppose adhesion and aggregation[7].

Platelets, with their ability of targeting vascular injury sites and releasing a variety of active substances during thrombogenesis, are a paradigm for a drug carrier in blood. Development of synthetic materials with the complex biochemical and physical attributes of natural cells may open new opportunities in medical therapy, but remains a difficult challenge. Reports have been published on synthetic blood cells [8, 9] and RGD-coated nanoparticles reproducing some of the functions exhibited by platelets during aggregation [10]. From the physical viewpoint, platelets are flexible and discoidal cell fragments, 2-4 μm in diameter and 0.5 μm in thickness. With respect to distinctive biological features, platelets express on their membrane surface an array of specific proteins that act as adhesive substrate receptors and are essential for localized hemostatic plug formation in areas of tissue damage. One of these receptors, the glycoprotein (GP) Ibα - a component of the GPIb-IX-V complex - is particularly relevant in that, by binding to the A1 domain of multimeric von Willebrand factor (VWF), endows platelets with the unique ability to tether to damaged vascular

surfaces under extreme conditions of shear stress. In this regard, GPIbα binding to the VWF A1 domain (VWF-A1) recapitulates one of the most distinctive platelet adhesive functions [11]. Here, we report the characterization of synthetic particles that distinctly and specifically target the receptor/ligand pair forming the GPIbα/VWF-A1 bond and exhibit enhanced adhesion to platelets and to a relevant platelet substrate under high shear stress.

As a first step of synthesis, we mimicked the size, discoidal shape and flexible nature of platelets. While fabrication of spherical particles using different polymers has been studied extensively, preparation of discoidal-shaped particles with such high flexibility is quite challenging. Fabrication of polymeric particles with non-spherical geometries has been established only recently with lithographic techniques and film stretching method [12-14]. Our process of making discoidal particles involved the following five steps: (i) the use of polymeric particles of appropriate size (1 μm); (ii) stretching them into a discoidal shape [15]; (iii) depositing alternate layers of oppositely charged proteins and polyelectrolytes using layer by layer technique - here, bovine serum albumin (BSA) or actin served as anionic layer and polyallylamine hydrochloride [16] as the cationic polyelectrolyte layer; (iv) cross-linking protein layers for stability; and (v) removing the polymeric core to yield highly flexible discoidal protein particles mimicking geometric features of human platelets and thus designated synthetic platelets (SPs; Fig. 1). Of note, use of actin as a structural protein of choice allows an even closer mimicry of natural platelets which possess a well-developed actin cytoskeleton (see supplementary information).

We then engineered the adhesive properties of SPs for selective recognition of platelet thrombi. For this purpose, we exploited the characteristics of the GPIbα/VWF-A1 bond, which initiates platelet tethering to vascular lesions exposed to high shear stress thus permitting subsequent interactions that promote stable platelet adhesion, activation and aggregation[17, 18]. We performed initial experiments with spherical polystyrene (PS) particles coated through physical adsorption with recombinant, disulfide-linked dimers of VWF-A1[19, 20] or chimeric dimers of the GPIbα amino terminal domain (GPIbαN) containing the VWF-A1 binding site[21-23]. Targeting with GPIbαN was envisioned to recapitulate platelet binding to immobilized VWF; conversely, by coating the GPIbα-binding VWF-A1 onto the surface of synthetic particles we intended to target platelets at sites of thrombus growth. We first tested the coated particles by perfusing each type over the respective counter-ligand immobilized onto the bottom surface of rectangular flow chambers. In all experiments, particles were added in defined numbers to a platelet-free suspension of red cells in buffer, with a packed red cell volume in the normal range (40-45%) for human blood. The efficiency of the interaction was assessed quantitatively by measuring the duration of particle-surface contacts and deriving the corresponding apparent dissociation rate constant (k_{off}) [24]. PS particles coated with VWF-A1 or GPIbαN at comparable surface density ($6-8 \cdot 10^3$ molecules/μm^2) had similar k_{off}, progressively increasing from ~0.5 to ~1.6 s^{-1} when the wall shear rate (γ_w) varied between 2 and $16 \cdot 10^3$ s^{-1}, but remaining unchanged at the higher γ_w of $24 \cdot 10^3$ s^{-1} (Fig. 2a). This behavior of the GPIbα/VWF-A1 bond - with faster off-rate under increasing tensile stress up to a limit value but greater resistance to dissociation when tensile stress exceeds the threshold - has been previously reported as typical of platelets tethering to multimeric VWF[11]. In this respect, therefore, synthetic particles coated with either moiety of the GPIbα/VWF-A1 receptor/ligand pair appear to reproduce a physiologic platelet property. Moreover, these findings indicate that particles coated with VWF-A1 may represent a new type of "platelets", not naturally existing, which can target exposed GPIbα.

Using reference PS particles coated with VWF-A1 at various surface densities, we then evaluated the effect of particle shape on the k_{off} of the interaction as a function of shear rate. At comparable targeting ligand densities, spherical particles (Fig. 2b) had a consistently

greater k_{off} (i.e. shorter lasting interactions resulting from a faster off-rate) than oblate-shaped ellipsoids (Fig. 2c). Moreover, using the latter particles, a sufficient number of experimental points was obtained at γ_w of $5 \cdot 10^3$ s^{-1} to demonstrate a significantly greater off-rate when the VWF-A1 surface density was $<1 \cdot 10^3$ as compared to $>2.5 \cdot 10^3$ molecules/μm^2 (Fig. 2c). It should be noted that there is a limitation to acquiring data at the higher γ_w values with particles in the lower range of targeting ligand surface density, as efficient adhesion is no longer supported. It is also noteworthy that, with particles coated with VWF-A1 above $2.5 \cdot 10^3$ molecules/μm^2 surface density, the off-rate appeared to reach the lowest possible level for a given γ_w condition (Fig. 2b and 2c). Since GPIbαN density on the bottom surface of the flow chamber was kept constant in all experiments, the result likely reflects formation of the maximum number of adhesive bonds that was possible for any given particle in relation to the γ_w value. The latter parameter defines a characteristic of the flow field that is proportionally related to flow velocity (influencing on-rate) and tensile stress on adhesive bonds formed (influencing off-rate), which ultimately limits adhesion efficiency.

We verified the validity of the results obtained with PS particles using SPs, shaped as oblate ellipsoids and mechanically flexible to mimic human platelets, compared to control polymer (PLGA) hard spheres coated with the same VWF-A1. The appropriate control for the effect of mechanical flexibility, comparing SPs and layer-by-layer fabricated PLGA spheres with the core dissolved, could not be performed because the latter particles no longer maintained their shape upon addition of an organic solvent. As with PS particles of similar shape, the k_{off} of SPs was considerably lower than that of spheres at all γ_w conditions tested (Fig. 2d). Of note, for both SPs and PLGA spheres the measured off-rate at any given γ_w value was greater than that of correspondingly shaped PS particles (compare Fig. 2d with Figs. 2b and 2c); nonetheless, there was the same tendency for the k_{off} to remain stable when γ_w increased over a threshold value ($>15 \cdot 10^3$ s^{-1} for spheres but between 5 and $10 \cdot 10^3$ s^{-1} for SPs). To test the stability of VWF-A1 adsorbed onto the surface of PLGA sphere, we measured the k_{off} of particles at the same position in the perfusion chamber after 2 or 22 minutes from the onset of flow at γ_w of $5 \cdot 10^3$ s^{-1}; the values were 4.85 and 8.66 s^{-1}, respectively. When particles perfused for 22 minutes on the same surface were re-tested on a fresh surface, the k_{off} measured 2 minutes after the onset of flow was 6.03 s^{-1}. This indicated that changes on the adhesive rather than the particle surface were more relevant for the observed off-rate increase, and that targeting molecules were adsorbed tightly onto the particle surface. Altogether, our findings indicate that the discoid (oblate ellipsoid) shape typical of human platelets is associated with better particle adhesion than a spherical shape regardless of material properties. In this regard, it is interesting to note that the off-rate values of human platelets adhering to VWF-A1 are of the same order of magnitude as those of PLGA spheres and SPs (Fig. 2e; compare with Fig. 2d) and significantly greater than those of PS particles (compare Fig. 2e with Figs. 2b and 2c). Thus, physical and chemical properties of particles and their surfaces, in addition to shape, influence the interaction with adhesive substrates exposed to flowing blood. Our present data cannot establish the respective relevance of shape and mechanical flexibility in determining the efficiency of particle adhesion, as we could not compare flexible particles of different shape (see above). Nonetheless, since the relative k_{off} difference between spherical and discoid rigid PS particles was similar to that between flexible discoid SPs and PLGA spheres, it appears that shape has a major influence on particle adhesion. This is likely because discoid particles can establish a greater contact area with the adhesive surface than spheres (Fig. 2f), and in addition non-spherical particles have a greater margination tendency in flowing blood [25, 26] facilitating interactions with the surface. Flexible particles may further increase their contact area by stretching onto the surface after the initial attachment, but the resulting effect on adhesion may be modest. Altogether, shape and mechanical flexibility may both contribute, albeit variably, to determining the adhesive properties of SPs.

After defining the structural and functional characteristics of SPs as compared to different microparticles, we evaluated their potential for specific targeting of platelet thrombi. To achieve this, we used an ex vivo perfusion model of platelet aggregation caused by the exposure of rapidly flowing blood to a surface coated with fibrillar collagen type I under high shear stress conditions. This model has been extensively characterized as likely representing the most physiopathologically relevant mechanisms involved in the platelet response to vascular injury, at least with respect to arresting hemorrhage that involves precapillary arterioles or contributing to thrombotic occlusion of stenosed atherosclerotic arteries [2, 17, 18]. To assess specificity, in addition to wild-type (WT) human VWF-A1 we coated microparticles with a single-residue mutant VWF-A1 in which Gly561 is replaced by Ser; this mutation causes a marked decrease in the efficiency of binding to GPIbα [25]. A substantial number of SPs coated with WT VWF-A1 became incorporated into platelet aggregates that accumulated over the collagen fibrils; depending on the targeting ligand coating density, the volume of SPs within these thrombi could amount to between 40 and 80 percent of the platelet volume (Fig. 3). Such a high incorporation is remarkable, particularly in view of the fact that the number of SPs added to blood ($1 \cdot 10^4/\mu l$) represented no more than approximately 2.5-7% of the platelet count ($1.5\text{-}4 \cdot 10^5/\mu l$ in human blood), indicating a high targeting efficiency mediated by the VWF-A1/GPIbαN bond. The biomechanical properties of SPs appear to be a relevant factor in the efficiency of targeting; indeed, the number of PLGA spheres that became incorporated into platelet aggregates was only approximately 1/8th of that of SPs coated with the same WT VWF-A1 at comparable surface density (Fig. 3). In addition to targeting efficiency, the VWF-A1-coated microparticles exhibited high specificity as replacement of the targeting WT ligand with the loss-of-function mutant resulted in a >95% reduction of microparticle incorporation into thrombi relative to platelets (Fig. 3). Altogether, the experimental results presented here support the concept that mimicking structural features of natural platelets coupled to the biomechanical properties of the VWF-A1/GPIbαN bond can significantly enhance thrombus targeting with microparticles.

The ability of SPs to target areas of vascular damage where platelets aggregate may have diagnostic and therapeutic applications. Indeed, because of their unique adhesive properties [6, 7], platelets are involved in several pathological processes - including myocardial infarction, stroke and peripheral vascular disease - that are among the most relevant causes of morbidity and mortality worldwide [2]. In most of these situations, efficient detection of localized venous and arterial thrombi may permit definitive diagnosis and identify a target for drug delivery in potentially life threatening situations. To facilitate imaging of thrombi, iron oxide nanoparticles for magnetic resonance imaging or other contrast media for state-of-the-art imaging techniques can be encapsulated within SPs. By virtue of the platelet targeting properties demonstrated here, imaging with these particles may provide accurate information on areas of the vasculature where lesions exist that elicit a thrombogenic response. With further research focused on detailed in vivo safety and efficacy studies, SPs may thus represent a new class of targeting agents engineered by mimicking natural platelets to improve targeting efficacy. Likewise, SPs may become platforms for the local delivery at high concentration of encapsulated antithrombotic and/or thrombolytic drugs, allowing prevention and treatment of diseases caused by arterial thrombotic occlusion with greater benefit and less severe side effects. Finally, SPs coated with VWF-A1 may prove useful for the treatment of bleeding by becoming incorporated into forming thrombi in an almost equal volumetric ratio with endogenous platelets augmenting thrombus volume and enhancing hemostatic efficiency. Considering the limited availability of adequate platelet preparations for transfusion purposes, the adjuvant hemostatic effect of SPs, which can be prepared in unlimited quantities, may prove useful. All potential diagnostic and therapeutic applications of SPs will require careful evaluation in future studies.

Experimental

Materials

PS spheres (1 and 3 µm) were from Polysciences (Warrington, PA). PLGA-2A (intrinsic viscosity 0.15-0.25) was from Lakeshore Biomaterials (Birmingham, AL). Poly(allylamine hydrochloride) (PAH; $M_w \sim$ 50 kDa), bovine serum albumin (BSA), bovine actin, heparin, 2-propanol, phosphate-buffered saline (PBS) tablets (pH 7.4) and polyvinyl alcohol (PVA, fully hydrolyzed) were from Sigma Aldrich (St. Louis, MO,). Tetrahydrofuran (THF), mineral oil, and glycerol were from EMD Biosciences (San Diego, CA). Dialysis cassettes (MWCO = 2500) were purchased Thermo Scientific (Hudson, NH).

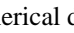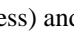### Fabrication of synthetic platelets

PS spheres were first stretched into oblate ellipsoidal templates using the film stretching method described by Champion et al [15]. Briefly, 10^8 PS spheres were embedded into a polyvinyl alcohol film (5 % w/v in water) containing 2% (v/v) glycerol as a plasticizer to facilitate stretching. The film was mounted on a two dimensional stretcher and stretched to twice the original length in oil at 125 °C (see Supplementary Information and Fig. S1). The film was then cut from the stretcher and, to minimize size and shape distribution, only a central circle of 3 cm diameter was used microparticle recovery; this was achieved by dissolving PVA in 15% isopropanol followed by 10 washing steps with 15% isopropanol for complete PVA removal. The resulting oblate ellipsoid-shaped template microparticles were suspended in distilled water or PBS. The template PS particles were then coated with alternate protein and polyelectrolyte layers using a layer-by-layer technique similar to one previously described[8]. First, a model protein, BSA, and a model polyelectrolyte, PAH, were used, each at a 2 mg/ml concentration for adsorption. BSA is negatively charged at the pH used, and PAH is a cationic polyelectrolyte; thus, alternate layers of the two held together by electrostatic interactions can be formed on the PS template particles. Seven bilayers were formed on the oblate ellipsoidal templates and they were cross-linked with glutaraldehyde intermittently to provide the required stability. The particles were then exposed to a solvent (a 2:1 THF/:isopropanol mixture) to dissolve the polymeric core; note that the choice of solvent is critical for achieving the desired particle morphology. The microparticles were finally washed 5 times with the solvent to ensure complete removal of the polymer. In subsequent preparations, BSA was replaced by actin. SPs were fluorescently labeled by standard succinimide ester chemistry, for example, NHS-rhodamine was conjugated to the amine groups present on the outer surface of SPs. To obtain scanning electron microscopy (SEM) micrographs of SPs fabricated with BSA or actin (Fig. S2), a 10-µl particle suspension sample was dispensed onto a SEM sample stub, vacuum dried and coated with palladium (Hummer 6.2 Sputtering System, Anatech Ltd., Union City, CA) for imaging with the Sirion 400 SEM (FEI Company, Hillsboro, OR) at an acceleration voltage of 5 kV.

Recombinant VWF-A1and GPIbαN and microparticle coating

A disulfide-linked, dimeric VWF fragment comprising residues 445-733 of the mature subunit (VWF-A1)[19]; and a chimeric protein comprising residues −2 to 288 of human GPIbα followed by 132 residues of the SV40 large T antigen (GPIbαN)[23] were expressed in stably transfected *D. melanogaster* cells, and purified to at least 90% homogeneity as judged by immunoblotting analysis. PS microparticles, PLGA spheres and SPs were incubated with targeting ligand at concentrations between 5 and 200 µg/ml in Hepes-buffered saline (HBS, pH 7.4 for VWF-A1 and pH 6.5 for GPIbαN) overnight at 4°C under constant rotation. PS microparticles were centrifuged at 5800 g for 5 minutes at room temperature (22- 25 °C). The coating solution was removed and replaced with HBS pH 7.4, and the pellet was resuspended by vortexing. This washing step was repeated once. PLGA

spheres and SPs were washed in a similar manner, but centrifuged at 600 g. Microparticles were counted in a flow cytometer (LSR II, BD Biosciences, Sparks, MD) calibrated with platelet suspensions of known count, as determined with a blood cell counter (Hemavet, Drew Scientific Inc., Dallas, TX). This method was in agreement with manual counting using a hemocytometer.

Flow cytometry

The surface density of targeting ligand on particles was quantified in a flow cytometer (LSR II BD Biosciences; see Supplementary Information and Fig. S3) using monovalent Fab fragments of the monoclonal antibodies NMC4, which binds to VWF-A1[27], and LJ-P3, which binds to GPIbαN[21]. These were labeled with Alexa Fluor 405 (Life Technologies, Grand Island, NY, USA) at fluorophore-to-protein (FTP) ratios of 1.7 and 2.9, respectively. Labeled antibody at the desired concentration was incubated with microparticles for 15 minutes before measuring binding. Uncoated particles and coated particles with no added antibody served as controls, and beads containing known amounts of fluorochrome [28] were used for instrument calibration. After subtracting uncoated from coated particle mean fluorescence, and assuming a 1:1 stoichiometry, the maximal binding (B_{max}) of monovalent Fab molecules derived from one-site nonlinear fitting of saturation dose-response curves was assumed to reflect the number of single VWF-A1 or GPIbαN reactive sites present on a particle surface, expressed as molecules per μm^2. The surface area of spheres was calculated using the mean diameter measured on SEM images; that of oblate ellipsoid was calculated by equating them to flat disks. The calculated surface area of SPs was increased by 57% to account for surface roughness (see Fig. 1c and Fig. S2). In order to estimate the percent increase in the area of a rough as compared to a smooth surface, we equated roughness to hemispherical domes (▲▲▲). As a first approximation in a two-dimensional system, the percent area increase was calculated from the difference between the semicircumference (roughness) and the diameter (smoothness) of a dome; for a unit diameter, this is (▬) x 100, or ~ 57%.

Blood preparation

For experiments with washed erythrocytes, blood was drawn from the antecubital vein of healthy, medication-free human volunteers who gave their informed consent according to an institutionally approved protocol incorporating the provisions of the Declaration of Helsinki. Blood was collected into syringes containing acid-citrate dextrose (ACD; 60 mM citric acid, 85 mM sodium citrate, 111mM dextrose, pH 4.5; 1 part ACD to 5 parts blood) to block coagulation. To prevent platelet activation, 10 μM prostaglandin (PG) E_1 was added along with 1.3 ATPase units/ml of the adenosine diphosphate (ADP) scavenger, apyrase (grade 7, Sigma; ATPase/ADPase ratio <2). To remove platelets, blood was centrifuged at 400 *g* for 10 minutes at room temperature; the resultant platelet-rich supernatant was removed - and kept for preparation of washed platelets, if needed - and replaced with an equivalent volume of Hepes/Tyrode buffer (17 mM Hepes, 130 mM NaCl, 2.7 mM KCl, 0.4mM NaH_2PO_4, 2.8 mM dextrose), pH 6.5, containing a reduced amount of apyrase (0.65 ATPase units/ml). After gentle mixing, the centrifugation was repeated twice at 2000 *g* for 10 min; each time, the supernatant was removed along with any platelets and white cells sedimented on top of the red cells, and replaced with Hepes/Tyrode buffer containing half the concentration of apyrase previously used. After the last centrifugation, washed cells were suspended in Hepes/Tyrode buffer, pH 7.4, containing 50 mg/ml BSA (Sigma); the packed red cell volume was adjusted to 45%, and the residual platelet count was not >20·10^3/μl.

For experiments of thrombus formation on collagen, blood was drawn into 40 μM PPACK (D-phenylalanyl-L-prolyl-L-arginine chloromethyl ketone dihydrochloride) to inhibit α-thrombin and prevent clotting without altering the plasma divalent cation concentration.

Quinacrine dihydrochloride (mepacrine, 10 μM final concentration) was added before perfusion to render the platelets fluorescent (excitation/emission wavelength: 485/518 nm).

Flow experiments

The adhesion of microparticles coated with VWF-A1 or GPIbαN to their complementary counter-ligand was studied in rectangular flow chambers with either constant or linearly increasing flow velocity from zero at the inlet to a maximum at the outlet; the latter is a modification of the Hele-Shaw flow described by Usami et al [29]. Glass coverslips coated with GPIbαN orVWF-A1 were assembled to form the lower surface of the chamber exposed to flowing blood, with a flow path height of 127 μm (determined by a silicone rubber gasket). The flow chamber was filled with HBS, pH 7.4, and mounted on the stage of an epifluorescence inverted microscope (Axiovert 135M, Carl Zeiss Inc, New York, NY). Blood was aspirated through the chamber at the desired velocity; microparticle adhesion was evaluated by direct visualization in real time and recorded digitally. Adhesion of microparticles incorporating a fluorescent dye (excitation/emission wavelength 580/605 nm) was evaluated with Metamorph software (Molecular Devices, Sunnyvale, CA) and translocation was tracked using a custom program originally designed for platelets [11]. The centroid (x, y) and area of newly arrested microparticles are recorded for each frame. The time within which the centroid is stationary or travels a distance of no more than one particle diameter from its original position is defined as residence time (Rtime). Following first order kinetics of dissociation, the k_{off} values are equal to the negative slope of the linear fit when plotting the cumulative frequency of microparticles as a function of Rtime. The k_{off} of platelet adhesion to VWF-A1 was measured with the same approach illustrated for microparticles, using washed platelets rendered fluorescent by the addition of 10 μM mepacrine added into the washed red cell suspension. Washed platelets were prepared as previously reported [18, 19] from platelet-rich plasma obtained as described under "blood preparation".

To study microparticle targeting of platelet aggregates forming in flowing blood, the bottom surface of a rectangular flow chamber with constant flow velocity was coated with fibrillar collagen type I [17, 18]. Whole blood with native divalent cation concentration and mepacrine-labeled platelets was perfused in a volume of 1.2 ml at $\gamma_w = 1500\ s^{-1}$. Thrombus formation was ceased by following the blood with Hepes buffer, pH 7.4, containing the same amount of mepacrine. Confocal image stacks were collected for platelets and microparticles separately and then processed using ImageJ image analysis software (National Institutes of Health of the USA; http://rsb.info.nih.gov/ij). Platelet aggregate and microparticle volumes were calculated from the sum of the areas covered by platelets or microparticles in each plane multiplied by the *z* distance (1 μm) between sections.

Supplementary Material

Refer to Web version on PubMed Central for supplementary material.

Acknowledgments

References

[1]. Thon JN, Italiano JE Jr. Seminars in Hematology. 2010; 47:220. [PubMed: 20620432]

[2]. Ruggeri ZM. Nature Medicine. 2002; 8:1227.

[3]. Semple JW, Italiano JE Jr. Freedman J. Nature Reviews Immunology. 2011; 11:264.

[4]. Gimbrone MA Jr. Aster RH, Cotran RS, Corkery J, Jandl JH, Folkman J. Nature. 1969; 222:33. [PubMed: 5775827]

[5]. Kaushansky K. Blood. 1995; 86:419. [PubMed: 7605981]

[6]. Ruggeri ZM, Mendolicchio GL. Circulation Research. 2007; 100:1673. [PubMed: 17585075]

[7]. Ruggeri ZM. Microcirculation. 2009; 16:58. [PubMed: 19191170]

[8]. Doshi N, Zahr A, Bhaskar S, Lahann J, Mitragotri S. Proceedings of the National Academy of Sciences USA. 2009; 106:21495.

[9]. Merkel TJ, Jones SW, Herlihy KP, Kersey FR, Shields AR, Napier M, Luft JC, Wu H, Zamboni WC, Wang AZ, Bear JE, DeSimone JM. Proceedings of the National Academy of Sciences USA. 2011; 108:586.

[10]. Bertram JP, Williams CA, Robinson R, Segal SS, Flynn NT, Lavik EB. Science Translational Medicine. 2009; 1:11ra22.

[11]. Savage B, Saldívar E, Ruggeri ZM. Cell. 1996; 84:289. [PubMed: 8565074]

[12]. Doshi N, Mitragotri S. Advanced Functional Materials. 2009; 19:3843.

[13]. Petros RA, DeSimone JM. Nature Reviews Drug Discovery. 2010; 9:615.

[14]. Meeuwissen SA, Kim KT, Chen Y, Pochan DJ, van Hest J. Angewandte Chemie. 2011; 123:7208.

[15]. Champion J, Mitragotri S. Proceedings of the National Academy of Sciences USA. 2006; 103:4930.

[16]. Johnston A, Cortez C, Angelatos A, Caruso F. Current Opinion in Colloid & Interface Science. 2006; 11:203.

[17]. Savage B, Almus-Jacobs F, Ruggeri ZM. Cell. 1998; 94:657. [PubMed: 9741630]

[18]. Ruggeri ZM, Dent JA, Saldivar E. Blood. 1999; 94:172. [PubMed: 10381510]

[19]. Ruggeri ZM, Orje JN, Habermann R, Federici AB, Reininger AJ. Blood. 2006; 108:1903. [PubMed: 16772609]

[20]. Reininger AJ, Heijnen HFG, Schumann H, Specht HM, Schramm W, Ruggeri ZM. Blood. 2006; 107:3537. [PubMed: 16449527]

[21]. Handa M, Titani K, Holland L, Roberts J, Ruggeri ZM. Journal of Biological Chemistry. 1986; 261:12579. [PubMed: 2943738]

[22]. Marchese P, Saldivar E, Ware J, Ruggeri ZM. Proceedings of the National Academy of Sciences USA. 1999; 96:7837.

[23]. Zarpellon A, Celikel R, Roberts JR, McClintock RA, Mendolicchio GL, Moore KL, Jing H, Varughese KI, Ruggeri ZM. Proceedings of the National Academy of Sciences USA. 2011; 108:8628.

[24]. Alon R, Chen S, Puri KD, Finger EB, Springer TA. The Journal of Cell Biology. 1997; 138:1169. [PubMed: 9281593]

[25]. Jordana A, David T, Homer-Vanniasinkamc S, Graham A, Walker P. Biorheology. 2004; 41:641. [PubMed: 15477670]

[26]. Decuzzi P, Pasqualini R, Arap W, Ferrari M. Pharmaceutical Research. 2009; 26:235. [PubMed: 18712584]

[27]. Celikel R, Ruggeri ZM, Varughese KI. Nature Structural Biology. 2000; 7:881.

[28]. Allen RD, Zacharski LR, Widirstky ST, Rosenstein R, Zaitlin LM, Burgess DR. The Journal of Cell Biology. 1979; 83:126. [PubMed: 511936]

[29]. Celikel R, Varughese KI, Madhusudan, Ware J, Ruggeri ZM. Nature Structural & Molecular Biology. 1998; 5:189.

[30]. Schwartz A, Gaigalas AK, Wang L, Marti GE, Vogt RF, Fernandez-Repollet E. Cytometry Part B: Clinical Cytometry. 2004; 57:1.

[31]. Usami S, Chen H, Zhao Y, Chien S, Skalak R. Annals of Biomedical Engineering. 1993; 21:77. [PubMed: 8434823]
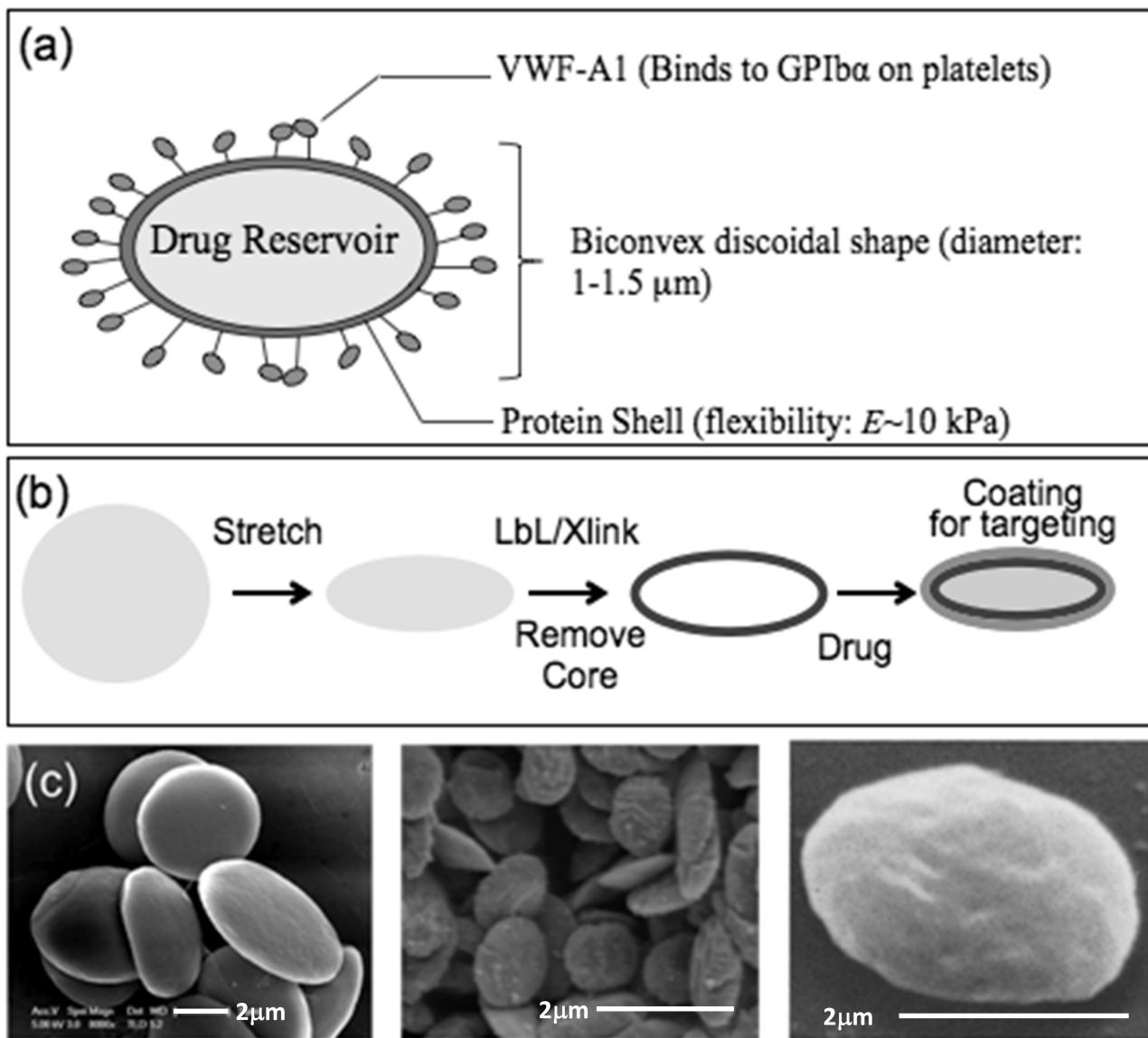
Figure 1. Fabrication of synthetic platelets
(a) Schematic representation of a synthetic platelet (SP) coated with VWF-A1 targeting drug delivery to platelets. (b) Sequential steps in SP fabrication. Spherical polymeric particles are first stretched into oblate ellipsoids. Proteins and polyelectrolytes are then coated on the templates using layer by layer technique followed by crosslinking of the layers and dissolution of the polymeric core to obtain SPs, which can then be loaded with drugs and coated with fluorophores and targeting ligands. (c) Scanning electron microscopy images showing (from left to right) oblate ellipsoidal polymeric templates; SPs; and natural platelets (reproduced from Ref. [26]).
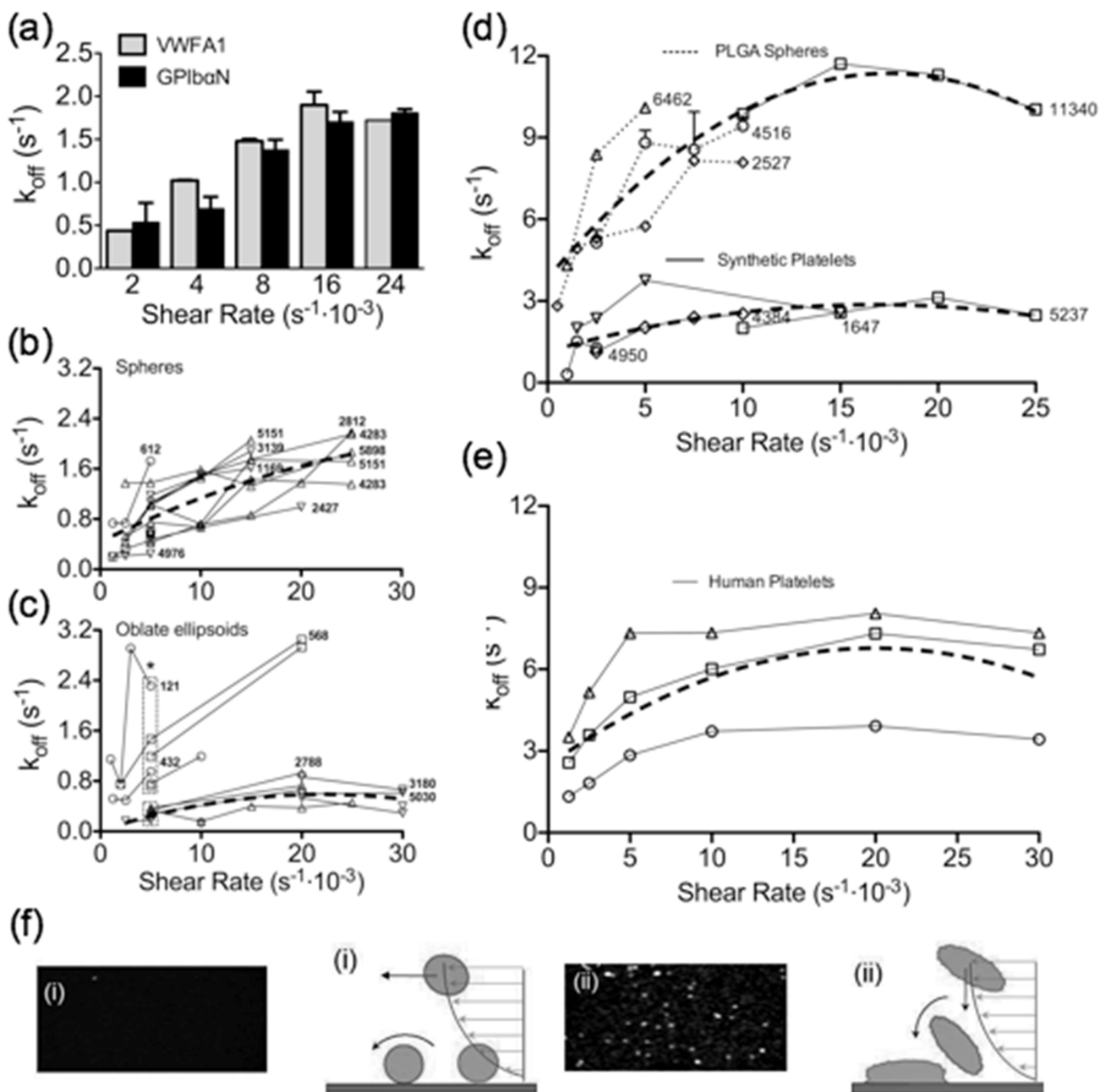
Figure 2. Targeting characteristics of particles coated with VWF-A1 and GPIbαN
(a) Fluorescent PS spheres coated with recombinant VWF-A1 fragment (50 μg/ml coating concentration; 6232 molecules/μm^2) or platelet GPIbαN (200 μg/ml coating concentration; 7856 molecules/μm^2) were added (1.5·10^3/μl) to a platelet-depleted washed human red cell suspension (40-45% packed red cell volume). This was perfused at the indicate wall shear rates (γ_w) through a flow chamber coated at the bottom with the complementary counter-ligand at comparable density (achieved with 20 μg/ml VWF-A1 and 10 μg/ml GPIbαN coating concentration). Adhesion was evaluated by measuring the dissociation rate constant (off-rate, k$_{off}$) of the particle-surface interaction. Grey bars: VWF-A1 particles perfused over immobilized GPIbαN (n=2); black bars: GPIbαN particles perfused over immobilized VWF-A1 (n=2). (b, c) Spherical (b) or discoid (c) PS particles were coated with VWF-A1 at

varying surface density achieved with different coating concentrations (circles, 5; squares, 16; upward triangles, 40; downward triangles, 100 μg/ml). The adhesion of particles ($1.5 \cdot 10^3/\mu$l) to GPIbαN was then evaluated at different γ_w values. Note (c) the lower off-rate at targeting molecule surface density $>2.5 \cdot 10^3$ as compared to $<1.5 \cdot 10^3$ molecules/μm^2 (experimental points within the lower or upper rectangle, respectively); *P=0.0153. The number of targeting molecules per μm^2 is indicated for all the particles on which it was measured. (d) Adhesion of PLGA spheres and synthetic platelets (particle count $1 \cdot 10^4/\mu$l) evaluated as described for PS particles of similar shape. The number of targeting VWF-A1 molecules per μm^2 is indicated for all the particles used. (e) Experiment performed and presented as in (d), but using fluorescent (mepacrine-loaded) washed human platelets from 3 different donors. Triangles, donor 1 ($20 \cdot 10^3/\mu$l); squares, donor 2 ($9 \cdot 10^3/\mu$l); circles, donor 3 ($13 \cdot 10^3/\mu$l). In (b-e), the thick broken lines represent the quadratic fitting of all points obtained in different experiments. (f) Schematic representation of the adhesion of hard PLGA spheres (i) or SPs (ii).
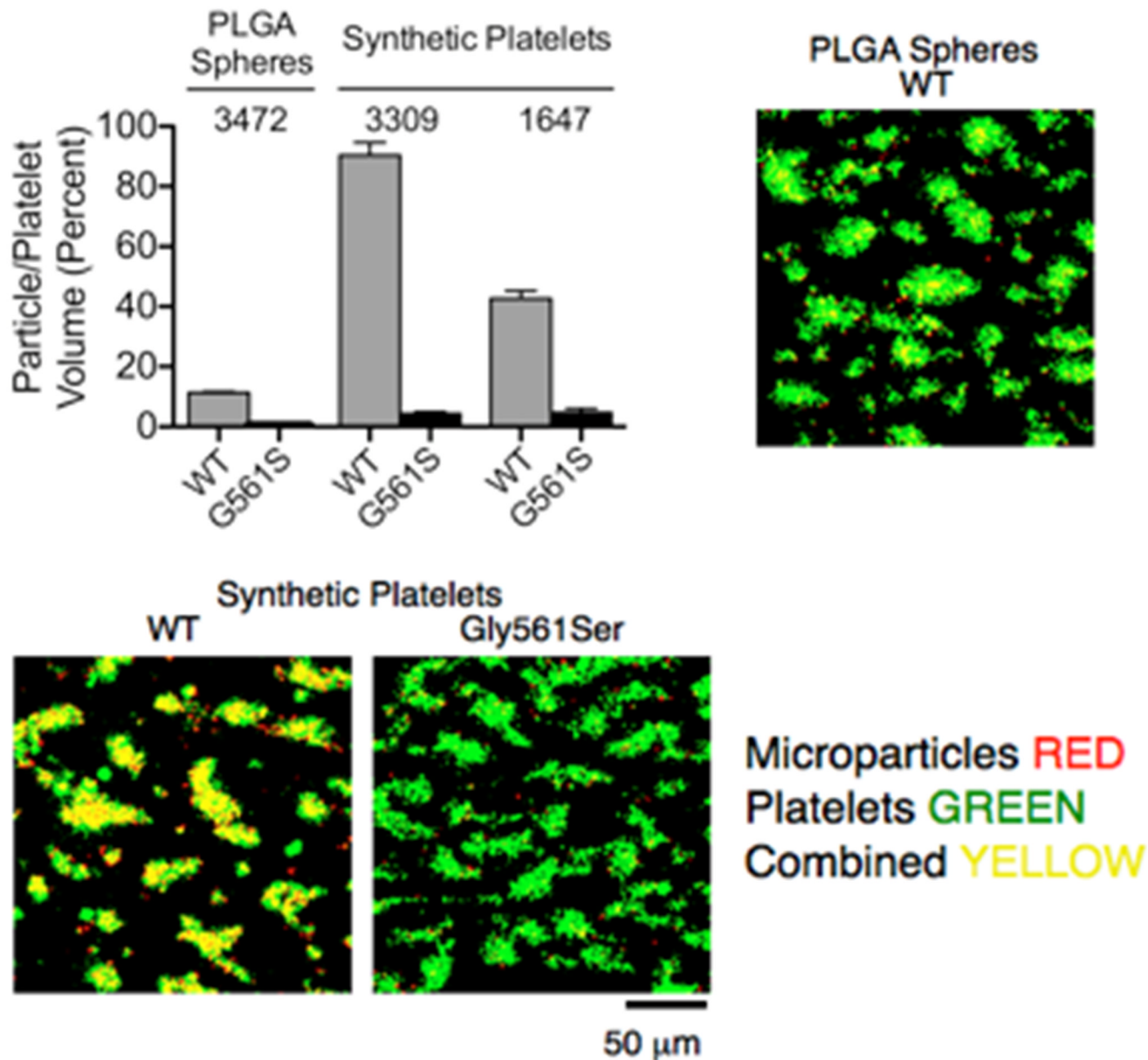
Figure 3. Platelet aggregate targeting in flowing blood using VWF-A1-coated SPs or PLGA spheres

Whole human blood containing 40 μM PPACK as anticoagulant and with mepacrine-loaded fluorescent platelets was perfused at γ of $1.5 \cdot 10^3$ s^{-1} w through a flow chamber coated onto the glass bottom surface with fibrillar collagen type I. A constant number ($1 \cdot 10^4/\mu$l) of fluorescent PLGA spheres or SPs coated with wild type (WT) or Gly561Ser mutant VWF-A1 was added to blood immediately before perfusion. At the end of perfusion, recorded in real time, series of confocal sections in the z axis were collected in the green and red fluorescence channels at three pre-selected positions on the chamber surface and used to reconstruct the volume of platelets and microparticles incorporated into the thrombi. The cumulative results of two separate experiments are presented as mean ± standard error of the mean (SEM). The surface density of targeting ligand is shown as molecules/μm^2; note that

the two experiments with SPs were performed using microparticles with different surface coating densities. The difference between PLGA spheres and both SP preparations was significant, as was the difference between the two SP preparations and the difference between each microparticle type coated with WT or Gly561Ser mutant VWF-A1 (all with $p<0.001$). Composite binary images (sum of confocal z-section stacks) show platelet (green) and particle (red) co-localization (yellow) within surface-attached thrombi.